ISBN: 978-3-95450-256-1 ISSN: 2673-5504 doi: 10.18429/JACoW-SRF2025-THB06C

FIRST BEAM COMMISSIONING OF THE bERLinPro SUPERCONDUCTING RADIO-FREQUENCY (SRF) PHOTOELECTRON GUN*

A. Neumann†, B. Alberdi, T. Birke, E.J. Brookes[1], J. Dube[1], P. Echevarria, D. Eichel, E. Ergenlik, R. Fleischhauer, A. Frahm, A. Heugel, F. Hoffmann, H. Huck, K. Janke, T. Kamps[1], G. Klemz, J. Knobloch [2], J. Kolbe, J. Kühn, S. Lederer, S. Mistry, N. Ohm, F. Pflocksch, H. Plötz, G. Rehm, S. Rotterdam, O. Schappeit, M. Schuster, H. Stein, A. Ushakov, J. Ullrich, J. Völker, C. Wang[2]
Helmholtz-Zentrum Berlin für Materialien und Energie, Berlin, Germany
[1]also at Humboldt Universität zu Berlin, Germany
[2]also at Universität Siegen, Germany
A. Galdi, Università degli Studi di Salerno, Italy
I. Will, Max Born Institut, Berlin, Germany

Abstract

After about a decade of research, development and construction work, the bERLinPro Energy Recovery Linac project at HZB changed over into the commissioning phase and started the operation of the SRF photo-injector with the injection line of the accelerator. This system had already produced beam from a metal photo-cathode in 2018 in a dedicated test environment and was assembled in the accelerator hall after a required refurbishment and repair program. The 1.3 GHz SRF gun successfully generated first photoemission beam from a high quantum efficiency (QE) Na-based multi-alkali photocathode. In this contribution, the results of the first two measurement campaigns will be shown, including a review of the SRF design, the RF commissioning, the cavity performance, especially with respect to dark current, the cathode quantum efficiency and lifetime, as well as the measured beam parameters.

INTRODUCTION

The SRF cavity based photo-injector [1] at bERLinPro [2] was initially designed to deliver a high power beam of about 2.5 MeV with an average current of 100 mA delivered in bunches of 77 pC filling every RF bucket at 1.3 GHz. This beam would have been transported and further accelerated by the booster module [3] to the injection energy of 6.5 MeV into the recirculator of the single loop high intensity Energy Recovery Linac (ERL). As a design and manufacture of such an high power system was regarded too risky, the injector was developed in several stages, whereas the first prototype featuring an high quantum efficiency photo-cathode in the green wavelength regime was designed to allow a maximum beam current of 5 mA, here limited by the power couplers. Table 1 gives an overview about the original design parameters and the potential performance of the current setup given the prototype SRF gun cavity and the 50 MHz photo-cathode laser for commissioning. An initially successful beam operation with a Cu photo-cathode with a dedicated beamline in a testbunker [4, 5] led finally to a failure of the transfer system with the Cs-K-Sb coated plug in 2018. A repair and refurbishment program was initiated [6], as the replacement cavity experienced a severe damage of the half-cell backwall during HPR assembly at the manufacturer. Following delays by the pandemic in 2020 to 2022, a large cyber-attack on HZB in 2023, shifted the completion of the injector assembly in the bERLinPro accelerator hall towards 2024 with first cooldown and RF operation. This was followed by a first beam trial in December 2024, which caused a failure of a power coupler's warm window, requiring replacement. Finally, first beam was achieved 28th of March 2025, with the first beam time ranging up to beginning of May, followed by a short beam time in July that year. Here, a power outage necessitated an early warm-up of the cryo-module and ended the experiments.

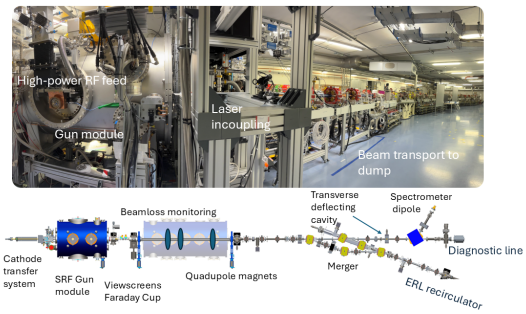

Figure 1: Picture and schematics of the bERLinPro injector. The Booster is here still replaced by quadrupole magnets.

Due to a redirection of HZB's research focus on 4th generation light sources by storage rings, the original goal of an high current ERL got out of reach and the whole bERLinPro facility became an application based accelerator laboratory under the new name SEALAB [7]. Still, ERL related research is as of submission of this manuscript part of SEALAB under the label bERLinPro, e.g. in the framework of the European Particle Accelerator Roadmap for High Energy Physics [8].

* Work supported by German Bundesministerium für Forschung, Technologie und Raumfahrt, Land Berlin, and grants of Helmholtz Association
† Axel.Neumann@helmholtz-berlin.de

ISBN: 978-3-95450-256-1 ISSN: 2673-5504 doi: 10.18429/JACoW-SRF2025-THB06C

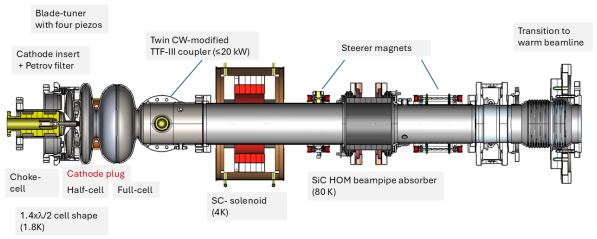

Figure 2: Layout of the SRF gun's cold string.

Figure 1 shows a picture of the injector of bERLinPro with the SRF gun module. Currently, the whole beam vacuum system, cathode transfer system, the cathode laser, LLRF system, magnets, diagnostics, machine protection system, beam loss monitoring, control system, cryogenics, cooling water and high power RF are installed. From the SRF systems only the SRF gun is assembled for beam operation, whereas the booster is currently in the cleanroom area for further assembly. In Fig. 2 the layout of the SRF gun coldstring is

Table 1: bERLinPro/SEALab Parameters

Parameter	ERL	Injector/UED
Beam energy (MeV)	50	6.5-10/2
I_{avg} (mA)	100	6-10/0.0025
Laser freq. (MHz)	1300	50, 1300
RF freq. (MHz)	1300	1300
ϵ_{norm} (mm mrad)	1 (0.6)	0.6/0.03
σ_t (ps)	2 (0.1)	0.02-2
Bunch charge (pC)	77	0.05-400

depicted. The system features a $1.4\times\lambda/2$ cell design, which is optimized for a high launch phase and thus emission field for peak-on-axis electric fields of 20-30 MV/m. The peak field seen by the electrons is shifted a bit downstream the cathode to limit field emission and also improve the focusing of the bunches by retraction of the cathode and an inclined back-wall of the half-cell. The cathode system is a modified version of the HZDR transfer system [9] using an SRF choke-cell to suppress any RF losses from the fundamental mode upstream in the cathode system. The cavity comes with two layers of magnetic shielding, a twin pair of TTF-III CW modified power couplers and a blade tuner system with four piezo elements, which is based on Cornell's ERL booster cavity design. The cavity is followed by a SC solenoid, two cold steerer magnets for both transverse planes surrounding the SiC HOM beamline absorber.

CAVITY PERFORMANCE AND DARK CURRENT

As the cavities for bERLinPro do not aim for highest field level, at the time of production [10] it was chosen to follow a conservative approach. The cavities were treated by BCP followed by 120 °C baking. This showed to already impact the cavity's Q-slope, but was not of a concern regarding the helium cooling budget of the cryo-plant and modules. In Table 2 an overview of the cavity RF design parameter and what could be measured or reconstructed of the manufactured resonator is given. For the second cavity, which is being installed, there is quite reliable data of the inner shape due to X-ray tomography performed after production and tuning [11], which revealed an over-tuning of the back-wall. As a result, it is merely flat, by that loosing its RF focusing ability and also resulting in a non-flat field distribution with an higher field level in the half-cell.

Figure 3 displays the intrinsic quality factor Q_0 over the peak on-axis accelerating field of the second gun cavity, which ended up being installed in the bERLinPro injector. Due to a damage during the final HPR process, the cavity

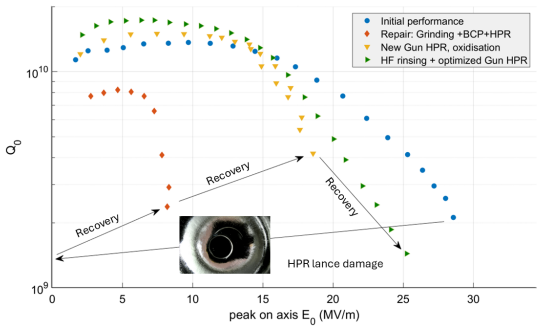

Figure 3: Evolution of cavity 1.1 Q_0 vs peak on axis field after production, damage during HPR assembly at the manufacturer and following HZB's repair program [6].

received a half-moon 50 µm deep dent next to the cathode opening, which made it practically unusable. A follow-up repair and refurbishment program, described here [6] allowed to mostly recover the cavity performance with potential kinetic beam energies up to 2.2 MeV. After this processing the cavity was also free of any measurable field emission. However, during the rather long assembly process and required installations in the accelerator hall eventually the cavity experienced a low level venting process with potential particulate transport. Unfortunately at this time, not all measured parameters were already written to the archiver of the control system. This was proven by the first field ramps in cold conditions, see Fig. 4, which shows the measured dark current from the cavity with a dose meter and also by focusing the unwanted beam on the first view-screen and Faraday Cup using the steerer magnets and the SC solenoid. This result is already after RF conditioning. It was shown, that the emitter persisted, but was able to be moved within the resonator, as the Fowler-Nordheim slope of the dark current curve changed during the processing. An example about that commissioning result is shown here [12].

The distributions of the dark current on the view-screen show the typical loop shapes, which result from the energy

ISBN: 978-3-95450-256-1 ISSN: 2673-5504 doi: 10.18429/JACoW-SRF2025-THB06C

Table 2: RF Design Parameters and the Values Estimated and Measured for the Prototype Cavity as Produced

Parameter	Design	As built
TM_{010} freq. (MHz)	1300	1300
$R/Q(\Omega)$ $\beta = 1$	150	132.5
$G(\Omega)$	174	154
P_{forward} max. (kW)	20	20
Q_{ext}	$3.6 \cdot 10^6$	$3 \cdot 10^7$
$\Delta f/\Delta P$ (Hz/mbar)	0	30-40
$\Delta f/\Delta l$ (MHz/mm)	1.6	1.3
$\Delta f/E_0^2$ (Hz/(MVm^{-1}))	3.2	3.8
E_{peak}/E_0	1.45	1.66
$B_{\text{peak}}/E_{\text{peak}}$ (mT/(MV/m))	2.27	2.18
E_{kin} (MeV)	3.5	1-2.5

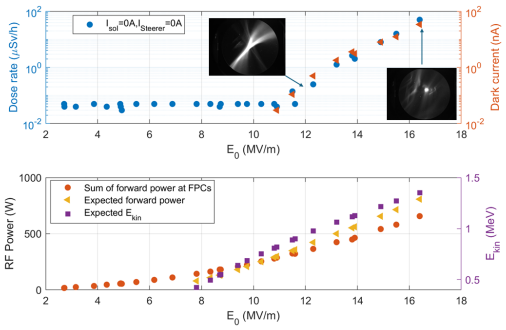

Figure 4: Measured radiation dose and dark current with first Faraday Cup vs. peak on axis field after RF processing of the emitters. The inserts show examples of dark current distributions focused with the SC solenoid on the first viewscreen. The lower plot depicts the measured RF power vs. expectation and level of kinetic beam energy to be reached.

distribution of the field emitted electrons subject to different focusing strength of the solenoid. A further more detailed analysis, measurement of the dark current energy by steerer and also scintillator systems and thus reconstruction of the emitters with tracking studies is planned for the future.

Here, also the impact of dark current electrons eventually back bombarding the photo-cathode is of interest and the contribution of the downstream traveling electrons on potential beam losses needs to be analysed. First work in this direction was done already here [13] and here [14].

The lower plot of Fig. 4 compares expected RF forward power to the actual measured values and the expected beam energy. The twin coupling scheme was balanced by a waveguide phase shifter and adjusting the individual external coupling quality factors to the same level with a VNA. Therefor, this hints already at a systematic error of the field's RF calibration, something we have also observed with the beam energy measurements.

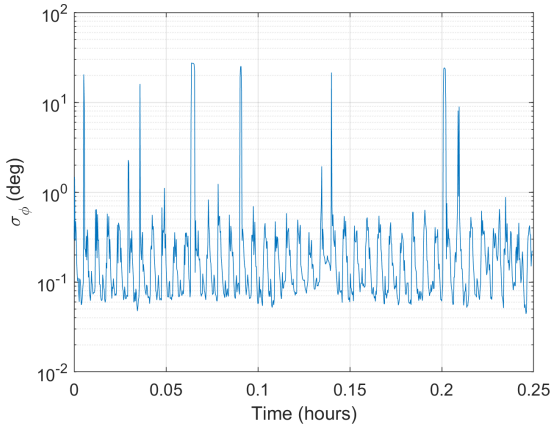

Figure 5: Cavity RF phase stability operated with a mTCA LLRF system while being on a regular pattern subject to strong kicks from the cryo-system.

LASER AND CATHODE PERFORMANCE

The cathode is driven by a 522 nm laser, which allows various pulse lengths, pulse energies and repetition rates up to 50 MHz. For the first measurements, we kept the laser mainly at 1 MHz repetition rate and 4 ps FWHM pulse length. More details are given here [12], but it is noteworthy, that the power stability of the laser was measured to be better than 0.6-1.5% for short term fluctuations. However, as the cryo-plant was going through its start-up phase in parallel, we have observed strong kicks eventually by the 4 K system to the cavity body, which causes a large detuning, reaching up to 50-100 Hz peak values with a semi-regular pattern. During these times, the phase field stability drops from 0.04 deg to 0.5 or even 15 deg rms. During these periods, a proper synchronisation of the mTCA LLRF system to the laser was not possible and any beam data taken was omitted. An example of these "cryo-kicks" on the cavity phase stability with time is given in Fig 5. The cause for this is still under investigation. External capacitive sensors gave a first hint towards the lower cryo-connection between coldbox and module.

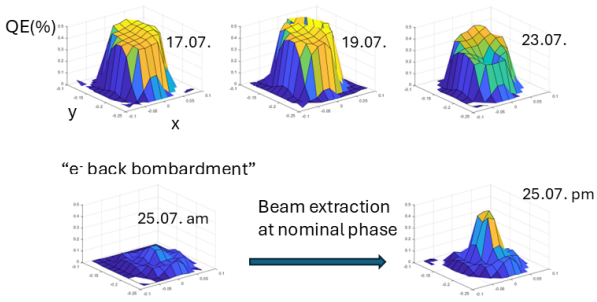

Figure 6: Evolution of the second Na-K-Sb photo-cathode's quantum efficiency maps with time.

For the beam operation of the SRF gun, a bialkali-antimonide Na-K-Sb [15] cathode was prepared in the cath-

ISBN: 978-3-95450-256-1 ISSN: 2673-5504 doi: 10.18429/JACoW-SRF2025-THB06C

ode lab, transported with a vacuum suitcase to the transfer system and then deployed to the cavity. The final position was determined by optical means of the cathode camera, electric contact measurements, the frequency shift of the TM_{010} passband modes and finally checked by interferometric methods. As the first photo-cathode was already discussed in [12] and more results will appear in future publications, we will discuss here mainly the second cathode.

The cathode started out with an high QE of about 6% and lost one order of magnitude during the transfer. This is already one order of magnitude better than with the first cathode, as the transfer had been improved since then. But even here, problems with the pincer, which grabs the cathode plug, required unnecessary handling steps, which have quite possibly impaired the cathode's QE.

Figure 7 depicts the QE maps of this cathode during the operation of the about two weeks short second beam-time. The QE was measured by the drain current of the cathode HV DC bias power supply, operated at 5 kV and a laser power of about 1 mW.

It can be seen, that the efficiency stayed rather constant in the first days and the distribution was rather uniform. Then first minima appear in the surface. Those might be caused by field emitters, which needs to be studied as mentioned before.

After one week (25.07) the quantum efficiency dropped from 0.5-0.6% by one order of magnitude. This happened, as after a short power outage we had to determine the RF phase window of emission again, which caused a full 360 deg RF phase scan and caused eventually back-bombardment of the cathode, by that affecting its emission properties. Interestingly, as we already saw with the first cathode [12], we observed a training or recovery of the cathode back to its original value especially at the location, from which the beam is emitted with now regular phasing between RF and laser.

This effect needs more study in the future, as it would increase potential lifetime of cathodes quite a lot, when they can be recovered within the SRF resonator.

FIRST BEAM

First beam was demonstrated end of March 2025 at a field level of E_0=10 MV/m. This field level was chosen to remain with a clean beam below any field emission onset. Figure 7 displays in the lower row on the left the electron beam focused on the first view-screen. The distribution left to it is by reflection of the laser beam. The stability of the latter with time demonstrated the good and stable pointing of the laser by the transport system from the above ground laser room to the cathode.

In later experiments, the laser was shaped by the institute's logo to image that via emitted electrons and proper solenoid settings on the screen as well. This was also helpful to determine the alignment errors of the solenoid, which showed to be small with a potential tilt towards the beam axis. This will be determined in more depth with future beam based alignment measurements.

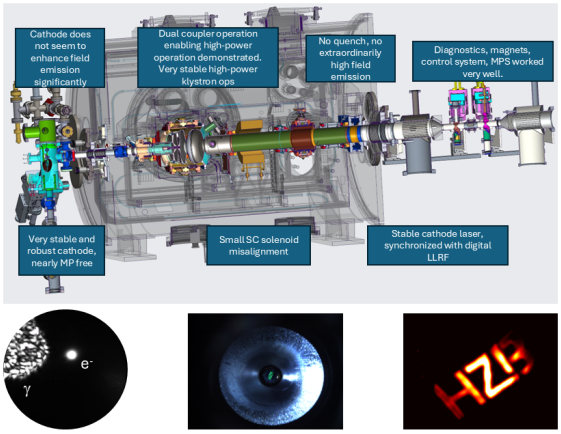

Figure 7: Overview of the SRF cryo-module with the main findings of the first two beam times. In the lower row, the pictures show the first beam on the viewscreen with a reflection of the laser beam on the upper left corner, the HZB logo imprinted by the laser on the photo-cathode (center picture) and transported via solenoid focussing and steering on the first viewscreen by the electron beam.

It is important to point out, that the cathode showed very few multipacting events, which usually occurs at very low field ≤1 MV/m and some few MV/m level due to the coaxial cathode channel. In the case here, it was only needed to once activate the DC bias to 3 kV, which suppressed any multipacting event. Here, we need to study, whether this is a positive aspect of the Sodium based cathode material compared to the often applied Caesium.

Longitudinal Beam Dynamics

To study the emission process and to evaluate the performance of an SRF gun cavity design, it is of paramount importance to analyze the longitudinal field dynamics of the cavity system. Here, in Fig. 8 the obtained kinetic energy of the beam, analyzed with the steerer magnets deflecting the beam on the viewscreen, is shown in relation to the emission phase between laser and RF field of the cavity.

We see the typical rather flat distribution for the low cavity field emission. However, the curves are below the expectation given by 3D CST [16] PIC simulations and other tracking studies. For the CST study the field distribution was even obtained by using the X-ray tomography model as boundary condition. This discrepancy hints at systematic errors with the measured RF field level, the assumed strength of the steerer magnets and the field distribution for tracking. Especially at lower fields deviations can have a large impact, as the phase slippage and turnover point to a synchronous phase between particle beam and RF can vary a lot with field level in this range.

ISBN: 978-3-95450-256-1 ISSN: 2673-5504 doi: 10.18429/JACoW-SRF2025-THB06C

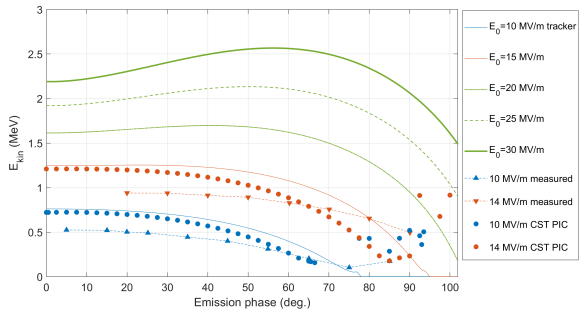

Figure 8: Kinetic energy of the electron beam vs. launch phase between laser and RF measured for two field levels ($E_0$10 and 14 MV/m compared to CST PIC tracking studies and results obtained by a self-written Runge-Kutta tracker.

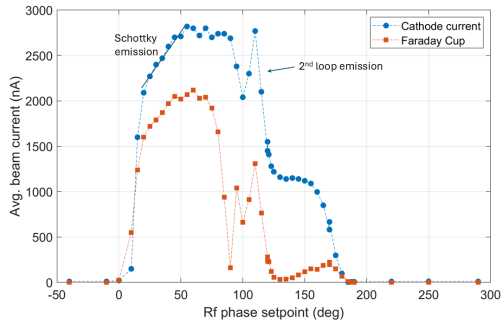

Figure 9: Average beam current measured vs. launch phase (LLRF setpoint phase) in the Faraday Cup and the cathode current system.

In Fig. 9 the emission process is studied to determine the onset phase for electrons being ejected from the cathode surface and the current level versus phase showing the launch field dependent Schottky emission [17] effect.

In this case a full 360 deg scan was necessary, as the phase information was lost after a power outage. Besides the Schottky range, the distinct peak at around 100 deg and above is caused by emitted particles being first completely decelerated within the half-cell, traveling back towards the cathode, to be accelerated again leaving the cavity, before they collide with the half-cell backwall or cathode. Some example trajectories of this rather narrow phase window can be seen in Fig. 10. However, there is still emission

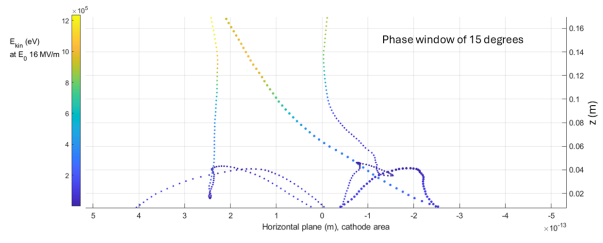

Figure 10: Tracking studies for electrons emitted at high launch phases (90-105 deg) forming a second loop within the half-cell before being extracted.

beyond that point to higher phases, which is not appearing in simulations and need to be understood better. Also, there is an offset between current measured at the Faraday Cup compared to the drain current at the cathode DC bias. This offset cannot be explained by beam loss and is possibly caused by a sampling effect of the latter measurement, which is better suited for close to DC measurements.

OUTLOOK

First beam was achieved with the bERLinPro SRF gun in the accelerator hall with a Na-K-Sb photo-cathode. The first measurement campaign, which was limited by field emission and the stability problem of the cryo-plant in field level, still leaves a large area of parameters to be studied in the future. In upcoming beam-times there is need to study both the longitudinal and transverse beam dynamics at the full range of field levels, especially going to the range towards 20 MV/m and potentially beyond. Also, the complete parameter space with respect to bunch charge, bunch length, beam current needs to be studied. We also plan to transport the beam further downstream to perform beam energy measurements with the spectrometer dipole and bunch length studies using the transverse deflecting cavity [18].

The here used cathode material showed a very promising performance and makes it potentially an ideal candidate for any SRF photo-injector driven facility. Studies within DC guns might also be of interest for some facilities. We need to further study the process of QE recovery and what circumstances in operation have impact on reducing the cathode performance and surface properties.

ACKNOWLEDGEMENTS

The authors would like to express their sincere acknowledgment to all current and former collaboration partners and co-workers of the former bERLinPro project, all accelerator division co-workers at HZB, who helped to bring this endeavor to a success, the SEALAB team, the support from facility management, especially Ralf Ziebell and our Gun Cluster partners at Helmholtz-Zentrum Dresden Rossendorf and DESY.

REFERENCES

[1] A. Neumann *et al.*, "Towards a 100mA Superconducting RF Photoinjector for BERLinPro", in *Proc. SRF'13*, Paris, France, Sep. 2013, pp. 42–49. https://jacow.org/SRF2013/papers/MOIOB02.pdf

[2] M. Abo-Bakr *et al.*, "Status Report of the Berlin Energy Recovery Linac Project BERLinPro", in *Proc. IPAC'18*, Vancouver, Canada, Apr.-May 2018, pp. 4127–4130. doi:10.18429/JACoW-IPAC2018-THPMF034

[3] A. Neumann *et al.*, "RF Conditioning of 120 kW CW 1.3 GHz High Power Couplers for the bERLinPro Energy Recovery Linac", in *Proc. SRF'21*, East Lansing, MI, USA, Jun.-Jul. 2021, pp. 216–220. doi:10.18429/JACoW-SRF2021-MOPTEV007

ISBN: 978-3-95450-256-1 ISSN: 2673-5504 doi: 10.18429/JACoW-SRF2025-THB06C

[4] J. Kuehn *et al.*, "A Cu Photocathode for the Superconducting RF Photoinjector of BERLinPro", in *Proc. IPAC'18*, Vancouver, Canada, Apr.-May 2018, pp. 1247–1250. doi:10.18429/JACoW-IPAC2018-TUPMF002

[5] A. Neumann *et al.*, "The BERLinPro SRF Photoinjector System - From First RF Commissioning to First Beam", in *Proc. IPAC'18*, Vancouver, Canada, Apr.-May 2018, pp. 1660–1663. doi:10.18429/JACoW-IPAC2018-TUPML053

[6] Y. Tamashevich *et al.*, "Damage recovery for srf photoinjector cavities", *Eng. Res. Express*, vol. 6, no. 2, p. 025 009, 2024. doi:10.1088/2631-8695/ad408a

[7] A. Neumann *et al.*, "bERLinPro Becomes SEALab: Status and Perspective of the Energy Recovery Linac at HZB", in *Proc. IPAC'22*, Bangkok, Thailand, Jun. 2022, pp. 1110–1113. doi:10.18429/JACoW-IPAC2022-TUPOPT048

[8] N. Mounet, *Vol. 1 (2022): European Strategy for Particle Physics - Accelerator R&D Roadmap*. CERN, 2022, pp. 80–84. doi:10.23731/CYRM-2022-001

[9] A. Arnold *et al.*, "Development of a superconducting radio frequency photoelectron injector", *Nucl. Instrum. Methods Phys. Res. A*, vol. 577, no. 3, pp. 440–454, 2007. doi:10.1016/j.nima.2007.04.171

[10] A. Burrill *et al.*, "Processing and Testing of the SRF Photoinjector Cavity for BERLinPro", in *Proc. IPAC'14*, Dresden, Germany, Jun. 2014, pp. 2484–2486, 2014. doi:10.18429/JACoW-IPAC2014-WEPRI005

[11] H.-W. Glock, J. Knobloch, A. Neumann, and A. VelÃ©z, "Industrial X-Ray Tomographie as a Tool for Shape and Integrity Control of SRF Cavities", in *Proc. SRF'21*, East Lansing, MI, USA, pp. 725–732, 2022. doi:10.18429/JACoW-SRF2021-THOTEV07

[12] T. Kamps *et al.*, "First beam commissioning of the hzb srf photoelectron gun", in *Proc. IPAC'25*, Taipei, Taiwan, Jun. 2025, pp. 1718–1721. doi:10.18429/JACoW-IPAC25-WECN2

[13] A. Neumann, Y. Tamashevich, and A. Ushakov, "Experimental and simulated dark current and beam loss studies for a srf photo-injector of an erl injector", in *Proc. IPAC'23*, Venice, Italy, May 2023, pp. 4525–4528. doi:10.18429/JACoW-IPAC2023-THPL044

[14] B. Alberdi-Esuain, A. Neumann, and T. Kamps, "Field emission and unwanted beam propagation simulations in the srf gun at sealab", in *Proc. IPAC'25*, Taipei, Taiwan, May 2025, pp. 1179–1181. doi:10.18429/JACoW-IPAC25-TUPM007

[15] S. Mistry, T. Kamps, J. Kühn, and C. Wang, "Multi-Alkali Antimonide Photocathode Development for High Brightness Beams", in *Proc. IPAC'22*, Bangkok, Thailand, Jun. 2022, pp. 2610–2613. doi:10.18429/JACoW-IPAC2022-THPOPT019

[16] *CST Studio Suite — 3ds.com*, https://www.3ds.com/products/simulia/cst-studio-suite, [Accessed 18-09-2025].

[17] Z. M. Yusof, M. E. Conde, and W. Gai, "Schottky-enabled photoemission in a rf accelerator photoinjector: Possible generation of ultralow transverse thermal-emittance electron beam", *Phys. Rev. Lett.*, vol. 93, no. 11, p. 114 801, 2004. doi:10.1103/PhysRevLett.93.114801

[18] G. Kourkafas, T. Kamps, B. Keune, and A. Neumann, "Transverse Deflecting Cavity for Longitudinal Beam Diagnostics at BERLinPro", in *Proc. LINAC'18*, Beijing, China, Sep. 2018, pp. 875–878. doi:10.18429/JACoW-LINAC2018-THPO083